Experimental control of a flexible link by the method of Controlled Lagrangian

Massoud Hemmasian Ettefagh [a*], **Mahyar Naraghi** [a], **Mojtaba Mahzoon** [b]

[a] Department of Mechanical Engineering, Amirkabir University of Technology, Tehran, Iran
[b] School of Mechanical Engineering, Shiraz University, Shiraz, Iran

A B S T R A C T

The Controlled Lagrangian method is a branch of energy shaping methods that is designed to control underactuated mechanical systems. The method employs the mechanical energy (kinetic energy plus potential energy) of an artificial Lagrangian system, that generates similar equations of motion to the original underactuated system, as the Lyapunov function. This paper presents an application of the Controlled Lagrangian method to control an underactuated flexible link, and the results of a theoretical study through simulations confirmed by the results from an experimental setup. It is shown that the method's performance is acceptable from a practical point of view as well as theoretical perspective. The simulations and the experimental results are presented in the sequel to validate the theoretical studies. The effect of changing controller gains on the designed controller performance is studied in more detail under the terms of the system's mechanical energy. Moreover, gain tuning is also performed to attain high quality performance in the experimental study by the aid of their influence in the system's energy. Comparison of the proposed method with the partial feedback linearization method shows the degree of robustness of the proposed method. The simplicity of the gain tuning shows that the method can be implemented conveniently to control mechanical systems.

1. Introduction

Robot manipulators play an essential role in almost all space projects. Given the cost of carrying materials to space skyrockets, reducing weight is vital for the continuation of space projects. In order to reduce weight in robot manipulators, it is necessary to use lighter materials and slender arms. With the reduction of arms thickness, the assumption of rigid links is no longer valid and

---

flexibility should be modeled in the dynamic behavior of manipulators. Methods of modeling flexibility in manipulators can be classified into two categories: numerical approaches and assumed mode methods [1]. The numerical approaches include finite deference and finite element methods [2] where the latter has shown its superiority over the finite deference method in terms of precision and computational burden [1].

A flexible link is an underactuated system, i.e. its number of actuators is strictly less than its degrees of freedom. The goal of controlling such system is to achieve good tracking of a reference path while minimizing the tip vibration. The nonlinear nature and the non-minimum phase behavior of flexible links render this task challenging and attractive for control theories [3]. The input shaping method [4] and direct strain feedback control scheme [5] are two of the pioneer works in this regard.

The Controlled Lagrangian method is an energy shaping method designed to control underactuated mechanical systems. It employs kinetic and potential energy shaping to control these systems. This method was initially introduced in [6-9]. It is shown that in order to stabilize an underactuated system in its unstable equilibrium point, shaping the potential energy alone is not sufficient and a modification in kinetic energy is also essential [8, 9]. Bloch et. al [8, 9] introduced a method to solve the nonlinear PDEs of kinetic energy and potential energy shaping. Auckly et. al [10-12] transformed the nonlinear PDEs of kinetic shaping to a system of linear PDEs, namely λ equations. Chang et. al. [13] introduced gyroscopic forces in the Controlled Lagrangian method to achieve more freedom in control gains, and then used this freedom to successfully stabilized more sophisticated systems such as Fruta pendulum. Donaire et al. [14] found a class of mechanical systems for which the solution of λ equations can be found readily. However, the mentioned class is very narrow and many mechanical systems fall out of it. In [15], the authors used energy shaping approach for a flexible joint with variable stiffness. The Controlled Lagrangian framework was also used in [16] and [17] for gait control of biped robots and lower-limb exoskeletons.

The aforementioned works were done in the Lagrangian framework. Similar works were done in the Hamiltonian framework and are referred to as *Interconnection and damping assignment passivity-based control* or IDA-PBC method [18-20]. The Controlled Lagrangian method and the IDA-PBC method have been shown to be equivalent [13] . Using the Controlled Lagrangian method, a simple control law for stabilizing an inverted cart pendulum system has been presented in [21]. In addition, the IDA-PBC method has been experimentally applied to a flexible link system [22]. For a class of underactuated mechanical systems such as Inertia Wheel, Haddad et al. [23] demonstrated that IDA-PBC is robust against external disturbances. Using a nonlinear PID as an outer loop controller, Donaire et al. [24] designed a robust IDA-PBC controller for a particular class of internal and external disturbances. In [25], the authors used an integral action to enhance the robustness of energy shaping method for underactuated systems.

In the present paper, we propose a control law for a flexible link system by the method of Controlled Lagrangian. Theoretical stability analysis and experimental validation are also provided. The effect of the controller's parameters on the system's performance is established via their influence on the system's mechanical energy. It is shown that the undesirable effect of structured uncertainties, including viscous damping, can be mitigated by this method. Gain tuning is employed to optimize performance in the sense of minimizing tip deflection and settling time in the simulation and experimental study by tuning only one coefficient.

The rest of the paper is organized as follows. In Section 2, the general formulation of Controlled Lagrangian method is presented. Next, the dynamical model of a flexible link system is obtained in Section 3. Section 4 employs the Controlled Lagrangian method to design a proper control law for the flexible link system. Simulation results and experimental results are discussed in Section 5. Conclusion and further remarks are presented in Section 6.

2. General method of Controlled Lagrangian

As mentioned in [10-13], the Controlled Lagrangian method is a control law strategy for underactuated systems with a regular Lagrangian. A *regular Lagrangian* system, by its definition, is a Lagrangian with the property of $\left[\frac{\partial^2 L}{\partial \dot{q}^i \partial \dot{q}^j}\right] \neq 0$. This expression is equivalent to the existence of a non-degenerative *inertia* tensor in *simple* mechanical systems. Unlike conventional potential energy shaping methods, Controlled Lagrangian method shapes the system's kinetic energy as well as its potential energy to obtain asymptotic stability in its intrinsically unstable equilibrium point. The main idea of the Controlled Lagrangian method is based on a simple fact: different lagrangians are able to produce same equations of motion (see [26] for more details). Different notations have been used by different authors, and in this paper, we adopt the notations and symbols of [13].

Simple Lagrangian systems are those whose Lagrangians ($L = T - U$) are quadratic with respect to velocity vector [27]. For a simple Lagrangian system, the triple (*L, F, W*) is defined as *Controlled Lagrangian system* where L is the Lagrangian of the system, F is the external force acting on the system and W is the *control bundle* of the system. The system is underactuated if the inequality rank $W < \dim Q$ (Q is the configuration space of the system) holds. Equations of motion of a Controlled Lagrangian system are given by [13],

$$\mathcal{EL}(L) \triangleq \frac{d}{dt}\frac{\partial L}{\partial \dot{q}} - \frac{\partial L}{\partial q} = F + [W]_{(n \times m)} u \tag{1}$$

where n = dim Q and m = rank W.

Using (1) for the regular Lagrangians L and $\hat{L}$, one can write,

$$0 = -(\mathcal{EL}(\hat{L}) - \hat{F}) + [\widehat{W}]\hat{u} \Rightarrow 0 = \left[\frac{\partial^2 L}{\partial \dot{q}\dot{q}}\right]\left[\frac{\partial^2 \hat{L}}{\partial \dot{q}\dot{q}}\right]^{-1}(\mathcal{EL}(\hat{L}) - \hat{F}) + \left[\frac{\partial^2 L}{\partial \dot{q}\dot{q}}\right]\left[\frac{\partial^2 \hat{L}}{\partial \dot{q}\dot{q}}\right]^{-1}[\widehat{W}]\hat{u}$$

Now, it is assumed that the two different regular Lagrangians (*L, F, W*) and $(\hat{L}, \hat{F}, \widehat{W})$ generate the same equations of motion. Hence, $\ddot{q} = \hat{\ddot{q}}$ must be valid for all $q \in Q$. In other words, the following expression is held for all $q \in Q$.

$$[W]u = \mathcal{EL}(L) - F - \left[\frac{\partial^2 L}{\partial \dot{q}\dot{q}}\right]\left[\frac{\partial^2 \hat{L}}{\partial \dot{q}\dot{q}}\right]^{-1}(\mathcal{EL}(\hat{L}) - \hat{F}) + \left[\frac{\partial^2 L}{\partial \dot{q}\dot{q}}\right]\left[\frac{\partial^2 \hat{L}}{\partial \dot{q}\dot{q}}\right]^{-1}[\widehat{W}]\hat{u} \tag{2}$$

For a simple mechanical system, (2) simplifies to [13],

$$[W]u = \left([C] - [M][\widehat{M}]^{-1}[\hat{C}]\right)\dot{q} + \{g\} - [M][\widehat{M}]^{-1}\{\hat{g}\} - F + [M][\widehat{M}]^{-1}\hat{F} + [M][\widehat{M}]^{-1}[\widehat{W}]\hat{u} \tag{3}$$

where [M] is the inertia tensor, [C] is the Coriolis and centripetal matrix, and $\{g\}$ is $\frac{\partial U}{\partial q}$ (effect of the potential energy). Since [W] is not a full rank matrix, it has a nonzero left annihilator. In other words, there exists a nonzero matrix $[W^{\perp}]$ with two properties: First, $T^*Q = W + W^{\perp}$ and second, $[W^{\perp}][W] = 0$. Note that T^*Q is the *tangent space* of Q (see [8] for definition of tangent space). These two conditions are satisfied by a matrix $W^{\perp}$ whose rows v are defined as [8],

$$\{v \in T^*Q | \forall \alpha \in W, \langle v, \alpha \rangle = 0\} \tag{4}$$

where $<\cdot,\cdot>$ is the inner product. Left multiplication of (3) by $[W^{\perp}]$ results in,

$$0 = [W^{\perp}]\left([C] - [M][\hat{M}]^{-1}[\hat{C}]\right)\dot{q} + [W^{\perp}]\left(\{g\} - [M][\hat{M}]^{-1}\{\hat{g}\}\right)$$
$$+ [W^{\perp}]\left([M][\hat{M}]^{-1}\hat{F} - F + [M][\hat{M}]^{-1}[\hat{W}]\hat{u}\right) \tag{5}$$

In order to satisfy (3) for all $\ddot{q}$, the control bundle $\hat{W}$ must be in the following form [13],

$$[\hat{W}] = \left[\frac{\partial^2\hat{L}}{\partial\dot{q}\dot{q}}\right]\left[\frac{\partial^2 L}{\partial\dot{q}\dot{q}}\right]^{-1}[W] \tag{6}$$

In this sequel we decompose the external forces F and $\hat{F}$ as,

$$F = F^q(q) + F^{v1}(q,\dot{q}) + F^{v2}(q,\dot{q}), \tag{7}$$

$$\hat{F} = \hat{F}^q(q) + \hat{F}^{v1}(q,\dot{q}) + \hat{F}^{v2}(q,\dot{q}), \tag{8}$$

in which $F^q(q), \hat{F}^q(q)$ are functions of coordinates q and are independent from velocity. The functions $F^{v1}(q,\dot{q})$, $\hat{F}^{v1}(q,\dot{q})$ are external forces due to viscous damping in the systems and other external forces that are first order with respect to the velocity vector $\dot{q}$ and functions $F^{v2}(q,\dot{q})$, $\hat{F}^{v2}(q,\dot{q})$ are external forces that are second order with respect to velocity vector $\dot{q}$. The reason that we distinguish between F^{v1} and F^{v2} is that these functions are being treated differently with respect to the left annihilator $[W^{\perp}]$. Using (6)-(8), Equation (5) reduces to three separate equations given as,

$$[W^{\perp}]\left[\left([C] - [M][\hat{M}]^{-1}[\hat{C}]\right)\{\dot{q}\} - F^{v2}(q,\dot{q}) + [M][\hat{M}]^{-1}\hat{F}^{v2}(q,\dot{q})\right] = 0, \tag{9}$$

$$[W^{\perp}]\left[\{g\} - [M][\hat{M}]^{-1}\{\hat{g}\} - F^q(q) + [M][\hat{M}]^{-1}\hat{F}^q(q)\right] = 0, \tag{10}$$

$$[W^{\perp}]\left[-F^{v1}(q,\dot{q}) + [M][\hat{M}]^{-1}\hat{F}^{v1}(q,\dot{q}) = 0\right]. \tag{11}$$

In local coordinations, these equations are expressed as,

$$W_{lk}^{\perp}\left[[ij,k]\dot{q}^i\dot{q}^j - m_{ka}\hat{m}^{ab}\widehat{[ij,b]}\dot{q}^i\dot{q}^j - F_k^{v_2} + m_{ka}\hat{m}^{ab}\hat{F}_b^{v_2}\right] = 0, \tag{12}$$

$$W_{lk}^{\perp}\left[\frac{\partial U(q)}{\partial q^k} - m_{ka}\hat{m}^{ab}\frac{\partial\hat{U}(q)}{\partial q^b} - F_k^q + m_{ka}\hat{m}^{ab}\hat{F}_b^q\right] = 0 \tag{13}$$

$$W_{lk}^{\perp}\left[\frac{\partial D}{\partial\dot{q}^k} - m_{ka}\hat{m}^{ab}\frac{\partial\hat{D}}{\partial\dot{q}^k} - F_k^{v_1} + m_{ka}\hat{m}^{ab}\hat{F}_b^{v_1}\right] = 0 \tag{14}$$

in which $[ij,k]$ denotes the Christoffel symbols of inertia matrix m_{ij}.

Equations (9)-(11) and their local representations (12)-(14) are known as *matching equations* [13]. The process of solving these equations is: First, (12) should be solved to determine all elements of $[\widehat{M}]$. The solution of $[\widehat{M}]$ shapes the kinetic energy. Then, the potential function $\widehat{U}$ is determined by shaping the potential energy via solving (13). Finally, the effect of external forces are compensated by solving (14).

In practice, due to the product of unknown $\widehat{m}^{ab}$ to its Christoffel symbols $\widehat{[ij,b]}$, (12) contains a set of first order nonlinear PDE's whose solutions can be quite prohibitive. However, the nonlinear PDEs (12)-(14) can be transformed to a set of triangular first order linear PDEs by using a new variable set, called λ. This variable is defined as [10]:

$$\lambda = \left[\widehat{M}\right]^{-1}[M].\tag{15}$$

Using (15), expressions (9)-(11) transform after some calculations, to the λ equations that in local coordinates are represented by [10]:

$$\frac{\partial\left(m_{\alpha i}\lambda_{\beta}^{i}\right)}{\partial q^{k}} - [\alpha k,i]\lambda_{\beta}^{i} - [\beta k,i]\lambda_{\alpha}^{i} - \widehat{G}_{ijk}\lambda_{\alpha}^{i}\lambda_{\beta}^{j} = 0\tag{16}$$

$$\lambda_{\alpha}^{k}\frac{\partial\widehat{m}_{ij}}{\partial q^{k}} + \frac{\partial\lambda_{\alpha}^{k}}{\partial q^{i}}\widehat{m}_{kj} + \frac{\partial\lambda_{\alpha}^{k}}{\partial q^{i}}\widehat{m}_{ki} = \frac{\partial m_{ij}}{\partial q^{\alpha}} - 2\widehat{G}_{ijk}\lambda_{\alpha}^{k}\tag{17}$$

$$\lambda_{\alpha}^{k}\frac{\partial\widehat{U}}{\partial q^{k}} = \frac{\partial U}{\partial q^{\alpha}} - F_{\alpha}^{(q)} + \lambda_{\alpha}^{k}\widehat{F}^{(q)}\tag{18}$$

$$F_{\alpha}^{(v1)} = \lambda_{\alpha}^{k}\widehat{F}^{(v1)}\tag{19}$$

In (16)-(19), the Latin indices vary from 1 to the total number of degrees of freedom (Dim Q) and the Greek indices vary from 1 to the number of underactuations (Dim Q − Dim W). These equations are triangular, that is (10) is solved first to determine λ_{i}^{α}, then, using λ, (17) is solved for $\widehat{m}_{ij}$, and finally, the shaped potential energy ($\widehat{U}$), is obtained from (18). Finally, (19) is used to transform external force $F_{\alpha}^{(v1)}$ to its equivalent in Lagrangian $\widehat{L}$.

Equations (16)-(19) indicate that the two Lagrangians (L, F,W) and $\left(\widehat{L},\widehat{F},\widehat{W}\right)$ generate the same equations of motion i.e. the equations of motion of Lagrangian (L, F, W) is equivalent to the equations of motion of Lagrangian $\left(\widehat{L},\widehat{F},\widehat{W}\right)$. During the solving process of (16)-(19), some arbitrary functions and constants emerge. These free functions and constants consist the control gains that are to be used to establish system stability. In the Controlled Lagrangian method, the Lyapunov candidate is the mechanical energy of the system ($\widehat{E} = \widehat{T} + \widehat{U}$). In this sequel, we employ the energy-momentum method to establish stability of the system. The general theory of the energy-momentum method with its details is given in [27]. In the case of a simple Lagrangian system, the energy-momentum method states that the system is stable at a specific point if the second variation of the mechanical energy function is positive-definite† at that point. In other terms, if all eigenvalues of the Hessian matrix for the mechanical energy function have positive real values, then the system is stable. For the mechanical energy function E, the second variation or Hessian matrix is defined as,

---

† In general, being definite is enough i.e. positive-definite or negative-definite. Here without loss of generality and for simplicity, positive-definiteness is assumed.

$$\delta^2 E_{2n\times 2n} = \begin{bmatrix} \left[\dfrac{\partial^2 E}{\partial q^2}\right]_{n\times n} & \left[\dfrac{\partial^2 E}{\partial q\dot{q}}\right]_{n\times n} \\[2ex] \left[\dfrac{\partial^2 E}{\partial \dot{q}q}\right]_{n\times n} & \left[\dfrac{\partial^2 E}{\partial \dot{q}^2}\right]_{n\times n} \end{bmatrix} \tag{20}$$

For a simple mechanical system, second variation matrix at the origin ($\boldsymbol{q = 0, \dot{q} = 0}$) reduces to,

$$\delta^2 E = \begin{bmatrix} \left[\dfrac{\partial^2 U}{\partial q^2}\right] & 0 \\[2ex] 0 & M \end{bmatrix} \tag{21}$$

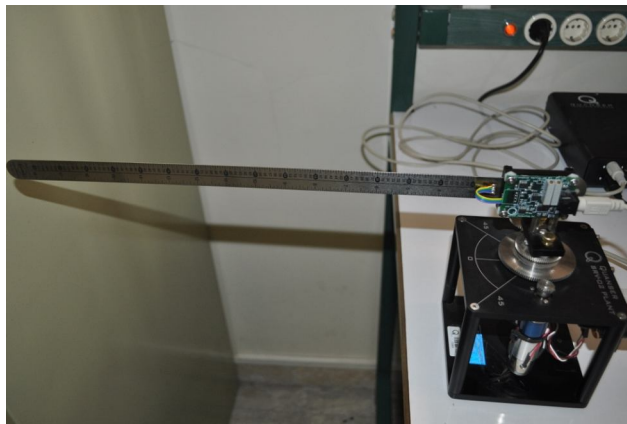where U is the potential function and M is the inertia tensor.

All of the free functions and constants of the solution for (16)-(19) must be chosen in an appropriate way to guarantee the positive-definiteness of the Hessian matrix for the energy function of $(\hat{L}, \hat{F}, \widehat{W})$. It should be mentioned here that the positive-definiteness of the Hessian matrix only guarantees stability of the system. To establish asymptotic stability, a proper dissipative control force $\hat{u}$ should be also employed.

By solving the matching equations (9), the control bundle of $\hat{L}$ in (6) will be determined. If m (dim W) is assumed to be 1, which means only one degree of freedom is actuated, then $[W]$ in (1) reduces to a column matrix whose elements are w_i, $i = 1, \dots n$. In this case, if $\hat{u}$ is chosen as,

$$\hat{u} = -c_0(w_1\dot{q}^1 + \cdots + w_n\dot{q}^n) , c_0 > 0 \tag{22}$$

then, it can be shown that system $(\hat{L}, \hat{F}, \widehat{W})$ is asymptotically stable. Finally, using (2), the equivalent control force u is computed such that the system (L, F, W) becomes asymptotically stable.

After determining $\hat{u}, \widehat{W}, \widehat{M}, \hat{F}$ from (10)-(15), the equivalent u for the Lagrangian system (L, F, W) is obtained from (3) as,

Fig 1: Experimental apparatus

$$u_{m\times1} = ([W]^T[W])^{-1}[W]^T(\mathcal{EL}(L) - F) - ([W]^T[W])^{-1}[W]^T\left[\frac{\partial^2 L}{\partial \dot{q}\dot{q}}\right]\left[\frac{\partial^2 \hat{L}}{\partial \dot{q}\dot{q}}\right]^{-1}(\mathcal{EL}(\hat{L}) - \hat{F})$$
$$+ ([W]^T[W])^{-1}[W]^T\left[\frac{\partial^2 L}{\partial \dot{q}\dot{q}}\right]\left[\frac{\partial^2 \hat{L}}{\partial \dot{q}\dot{q}}\right]^{-1}[\hat{W}]\hat{u}.$$

(23)

3. Dynamical model of the flexible link

A common procedure to model the dynamical behavior of flexible links is to employ the assumed mode method [1, 22]. In the present paper, Euler-Bernoulli beam theory is used to model a flexible link with one degree of freedom. In this method, elastic deformation of the link $w(x,t)$ is defined as a superposition of an infinite number of modes where time and spatial variables are separable as,

$$w(x,t) = \sum_{i=1}^{\infty} \psi_i(x)F_i(t)$$

where $\psi_i(x)$ and $F_i(t)$ are the *i-th* mode shape and *i-th* mode amplitude.

In order to obtain a set of finite-dimension ODEs, n modes are assumed. The Lagrange Equations result in a dynamical system which consists of $n+1$ second order differential equations [22, 28]:

$$\begin{bmatrix} J & 0 \\ 0 & J_{tot} \end{bmatrix}\begin{Bmatrix} \ddot{q}_i(t) \\ \ddot{q}_0(t) \end{Bmatrix} + \begin{bmatrix} K_f & 0 \\ 0 & 0 \end{bmatrix}\begin{Bmatrix} q_i(t) \\ q_0(t) \end{Bmatrix} = \begin{Bmatrix} \psi(0) \\ 1 \end{Bmatrix}u$$

(24)

where J_{tot} is the total inertia around the axis of rotation, J is the inertia matrix regarding to the generalized flexible coordinates, $q_i(t)$ and $q_0(t)$ are the rigid generalized coordinate, K_f is the stiffness matrix that depends on the link's elasticity and it can be defined as $K_f = diag(\omega_i^2)$, where ω_i is the natural frequency of the *i-th* mode. Finally u represents the applied control torque. Defining the tracking errors as $\tilde{q} = q - q_d$, where q_d is the desired trajectory for the flexible link such that $\ddot{q}_d = 0$ and $q_d = 0$, the dynamical equations result in,

$$\begin{bmatrix} J & 0 \\ 0 & J_{tot} \end{bmatrix}\begin{Bmatrix} \ddot{\tilde{q}}_i(t) \\ \ddot{\tilde{q}}_0(t) \end{Bmatrix} + \begin{bmatrix} K_f & 0 \\ 0 & 0 \end{bmatrix}\begin{Bmatrix} \tilde{q}_i(t) \\ \tilde{q}_0(t) + q_{0d} \end{Bmatrix} = \begin{Bmatrix} \psi(0) \\ 1 \end{Bmatrix}u$$

(25)

For system (25), the kinetic and potential energy are given as

$$T = \frac{1}{2}J_{tot}\dot{q}_0^2 + \frac{1}{2}\{\dot{q}_i(t)\}^T J \{\dot{q}_i(t)\}$$

(26)

$$U = \frac{1}{2}\{q_i(t)\}^T K_f \{q_i(t)\}$$

(27)

Assuming the first flexible mode, it is more convenient to change the coordinates from q_i to θ and α, where θ is the link angle and α is the tip deflection angle ($\alpha = \tan\frac{D}{L} \approx \frac{D}{L}$). Hence, the kinetic and potential energy of a single flexible link reduce to,

$$T = \frac{1}{2}J_{hub}\dot{\theta}^2 + \frac{1}{2}J_{link}(\dot{\theta} + \dot{\alpha})^2,$$

(28)

$$U = \frac{1}{2}K_{st}\alpha^2.$$

(29)

87

where, J_{hub} is the moment of inertia of the rotational base, $J_{link} = \frac{1}{3}mL^2$ is the moment of inertia of the flexible link, and *Kst* is the stiffness coefficient that is determined from the first flexible shape mode.

Here (28) and (29) are considered as the model that is used to design the controller. The corresponding system's equations of motion are obtained by applying (1) on (28) and (29) as,

$$\begin{bmatrix} J_{link} & J_{link} \\ J_{link} & J_{link} + J_{hub} \end{bmatrix} \begin{bmatrix} \ddot{\alpha} \\ \ddot{\theta} \end{bmatrix} + \begin{bmatrix} K_{st}\alpha \\ 0 \end{bmatrix} = \begin{bmatrix} 0 \\ 1 \end{bmatrix} u. \tag{30}$$

While the control input in (30) is the torque, the control input of the laboratory experimental apparatus is the input voltage to a DC motor. The relation between these two quantities, based on the apparatus specifications, is given by [29] as,

$$u_{output} = \frac{\eta_m \eta_g K_t K_g}{R_m} V_m - \frac{\eta_m \eta_g K_t K_g^2 K_m}{R_m} \dot{\theta}. \tag{31}$$

Thus, the equations of motion for the flexible link system is [29],

$$J_{link}\ddot{\alpha} + J_{link}\ddot{\theta} + K_{st}\alpha = 0, \tag{32}$$

$$J_{link}\ddot{\alpha} + (J_{link} + J_{hub})\ddot{\theta} + \underbrace{\left(B_{eq} + \frac{\eta_m \eta_g K_t K_g^2 K_m}{R_m} \right)}_{D_{eq}} \dot{\theta} = \frac{\eta_m \eta_g K_t K_g}{R_m} V_m. \tag{33}$$

Where the description and values of constants in (32) and (33) are given in Table 1.

Table 1. Specifications of laboratory flexible link apparatus [29]

Property	Value	Property	Value
Link mass, m	65 [gr]	Moment of inertia of base devices, J_{hub}	2.086 [gr.m²]
Link length, l	16.5 [in]	Motor armature resistance, R_m	2.6 [Ω]
Total gear ratio, K_g	70	Motor back-EMF constant, K_m	0.00767 [V.s/rad]
Gearbox efficiency, η_g	0.9	Motor torque constant, K_t	0.00767 [N.m/A]
Motor efficiency, η_m	0.69	Viscous damping coefficient, B_{eq}	0.004 [$\frac{N.m.s}{rad}$]
Link stiffness, K_{st}	1.66 [$\frac{N.m}{rad}$]		

4. Controller design

The control bundle, with respect to voltage V_m as the controller input, is obtained from (32) and (33) as,

$$W = \begin{bmatrix} 0 \\ \frac{\eta_m \eta_g K_t K_g}{R_m} \end{bmatrix} \tag{34}$$

Additionally, for this particular system we have $F^{v2}(q, \dot{q}) = 0$; therefore, solving (16) and (17) indicates that elements of the inertia tensor $\widehat{M}$ are arbitrary constants. For simplicity, inverse of the inertia tensor is assumed to be,

$$\widehat{M}^{-1} = \begin{bmatrix} a_1 & a_2 \\ a_2 & a_3 \end{bmatrix} \tag{35}$$

Consequently, (12) in the absence of external forces ($F^q(q) = 0$) reduces to:

$$(a_1 + a_2)\frac{\partial \widehat{U}}{\partial \alpha} + (a_2 + a_3)\frac{\partial \widehat{U}}{\partial \theta} - \frac{K_{st}}{J_{link}}\alpha = 0. \tag{36}$$

The general solution of (36) is,

$$\widehat{U} = \frac{1}{2}\frac{K_{st}}{(a_1 + a_2)J_{link}}\alpha^2 + F_1\left(\theta - \frac{a_2 + a_3}{a_1 + a_2}\alpha\right), \tag{37}$$

where $F1(.)$ is an arbitrary smooth function of its argument.

According to energy-momentum (21), $F_1(\cdot)$ is used to preserve stability; therefore, the second derivative of $F_1(\cdot)$ should be nonzero. The simplest choice for this function is,

$$F_1 = \frac{1}{2}\varepsilon\left(\theta - \frac{a_2 + a_3}{a_1 + a_2}\alpha\right)^2 \tag{38}$$

Thus, the second variation of the system $(\widehat{L}, \widehat{F}, \widehat{W})$ (Hessian Matrix) is:

$$\delta^2\widehat{E} = \begin{bmatrix} \dfrac{K_{st}}{(a_1 + a_2)J_{link}} + \varepsilon\left(\dfrac{a_2 + a_3}{a_1 + a_2}\right)^2 & -\varepsilon\dfrac{a_2 + a_3}{a_1 + a_2} & 0 & 0 \\ -\varepsilon\dfrac{a_2 + a_3}{a_1 + a_2} & \varepsilon & 0 & 0 \\ 0 & 0 & \dfrac{a_3}{a_1 a_3 - a_2^2} & \dfrac{-a_2}{a_1 a_3 - a_2^2} \\ 0 & 0 & \dfrac{-a_2}{a_1 a_3 - a_2^2} & \dfrac{a_1}{a_1 a_3 - a_2^2} \end{bmatrix} \tag{39}$$

In order to guarantee the positive definiteness of the Hessian Matrix (39), one can easily check that the following conditions must be satisfied:

$$a_1, a_3, \varepsilon > 0 \; ; a_1 + a_2 > 0 \; ; a_1 a_3 - a_2^2 > 0 \tag{40}$$

The control bundle $\widehat{W}$ is then obtained by substituting $[\widehat{M}]$ from (35) into (6) as:

$$\widehat{W} = [\widehat{M}][M]^{-1}W = \frac{\eta_m\eta_g K_t K_g}{R_m J_{hub}(a_1 a_3 - a_2^2)}\begin{bmatrix} -(a_2 + a_3) \\ a_1 + a_2 \end{bmatrix} = \begin{bmatrix} P_\alpha \\ P_\theta \end{bmatrix} \tag{41}$$

Next, the dissipation function is obtained by employing (22) as:

$$\hat{u} = -c_0\left(\frac{\eta_m\eta_g K_t K_g}{R_m J_{hub}(a_1 a_3 - a_2^2)}\right)\left((a_1 + a_2)\dot{\theta} - (a_2 + a_3)\dot{\alpha}\right). \tag{42}$$

In order to compensate D_{eq} in (33) in the control algorithm, we use (19) to determine $\widehat{F}^{v1}$ from,

$$F^{v1} = \begin{bmatrix} 0 & 0 \\ 0 & D_{eq} \end{bmatrix}\begin{Bmatrix} \dot{\alpha} \\ \dot{\theta} \end{Bmatrix} \tag{43}$$

in the control algorithm (23). Finally, the desired control input (in volts) for the flexible link is obtained by substituting (35), (37) and (41)-(43) into (23).

5. Simulation and experimental results

To demonstrate the performance of the proposed controller, a series of simulations and experiments are presented in this section. The laboratory apparatus (Figure 1), fabricated by Quanser Consulting Inc., is a thin steel ruler that moves in the horizontal plane by the action of a DC motor. The angular position of the link θ is measured by a US Digital 1024-bit encoder and its tip deflection angle α is measured by means of a strain gauge that is placed near the base. The method of measuring the tip deflection from the strain gauge is illustrated in the appendix. Table 1 shows the specifications of the experimental device. The control gains to be determined for the suggested controller are $a_1, a_2, a_3, \varepsilon$ and c_0. These five control gains have quite different roles in the control process: a_1, a_2 and a_3 shape the kinetic energy, ε shapes the potential energy and c_0 indicates the dissipation rate of energy from the system. In all of the simulations and experiments, the three gains a_1, a_2 and a_3 do not change. Equations (38) and (42) indicate that these three coefficients play the interconnection role between θ, α and their derivatives. The only restriction of finding these gains stems from (40). Therefore, any combination of a_1, a_2 and a_3 that satisfies (40) is able to stabilize the system. The subject of this paper is to deal with ε and c_0 from system's mechanical energy perspective as well as the effect of these variables on the system's performance. In this section, the effects of ε and c_0 on the controller performance such as overshoot and settling time are examined by means of simulation and experiment. Moreover, the difference between simulations and experiments are discussed. Finally, effect of these coefficients on the system's mechanical energy and stability is examined here.

Any combination of $a_1, a_2, a_3, \varepsilon$ and c_0 that satisfies (22) and (40) provides asymptotical stability for the system. Further tuning of these values leads to the improvement of system's performance. It can be seen from (37) that $a_1.a_2.a_3$ provides interconnection for potential energy function $\hat{U}$, so their effect on system's performance is nonlinear which makes them inappropriate for improvement in the system's performance. On the other hand, ε and c_0 could be considered as the stiffness and damping coefficients of Lagrangian $\hat{L}$. The linear effect of ε and c_0 on the system's energy, which can be seen in (22) and (38), makes them appropriate for the performance improvement.

The inherent robustness of the Controlled Lagrangian method is discussed in [30]. It is shown that for structured uncertainties $\tilde{M}, \tilde{C}, \tilde{g}$, the uncertain dynamical system,

$$([M] + [\tilde{M}])\ddot{q} + ([C] + [\tilde{C}])\dot{q} + \{g\} + \{\tilde{g}\} = u \tag{44}$$

remains stable as long as its associated Hessian matrix remains positive definite. The Hessian matrix of the uncertain system is [30],

$$\delta^2 \hat{E} = \begin{bmatrix} \left[\dfrac{\partial^2 \hat{U}}{\partial q^2} + \dfrac{\partial}{\partial q}\left(\hat{M} M^{-1} \dfrac{\partial \tilde{U}}{\partial q} \right) \right] & 0 \\ 0 & \hat{M} + \hat{M} M^{-1} \tilde{M} \end{bmatrix} \tag{45}$$

Uncertain parameters, including flexibility coefficient K_{st} and mass distribution of the beam, pose their effects on $\tilde{U}, \tilde{M}$ and $\tilde{C}$. Unknown damping coefficient of the joints and other dissipative effects affect the equations of motions through (43). If the tuning parameters $a_1, a_2, a_3, \varepsilon$ keep eigenvalues of the nominal Hessian matrix well far from the origin, the negative

effect of uncertainties and disturbances does not change the sign of eigenvalues, which leads to stability of the system.

The control gains are selected as $a_1 = 108$, $a_2 = -100$, $a_3 = 101$, $\varepsilon = 30$, $c_0 = 0.2$. It can be shown easily that these values satisfy (22) and (40). The controller goal is to regulate the tip's deflection (α). Figure 2 presents simulation and experimental results for the main control gains where the trajectories show tip total angle ($\theta + \alpha$). While the simulation shows no overshoot, the experimental result displays about 8 percent (4 degrees) overshoot. Also, the settling time is slightly better in the simulation than in the experiment. The main cause of the discrepancy between the simulation and experimental result is the uncertainty in the modeling and the effect of the non-modelled dynamics. Such an inaccuracy deteriorates the controller performance and causes overshoot and a longer settling time.

As it can be seen in (37)-(40), ε is a weighting parameter for shaping the potential energy of the equivalent system $\hat{L}$. According to (38), this parameter controls the amount of artificially injected potential energy into the system $\hat{L}$. In other words, one can assume $\frac{1}{2}\varepsilon\left(\theta - \frac{a_2+a_3}{a_1+a_2}\alpha\right)^2$ as the potential energy of an artificial spring where its stiffness is equal to ε. Any variation in ε changes the amount of stored energy in $\hat{L}$. Since L and $\hat{L}$ generate same equations of motion, any variation in energy content of $\hat{L}$ has its direct effect on the equations of motion of the original system L. Equation (23) makes the connection between $\hat{L}$ and the required control effort u, and hence, it can be seen from (23) that the value of ε controls the maximum input effort u. In the presence of input constraint, one can tune ε to adjust the controller's effort well below the constraint. This prevents any saturation in the system's input. Figures 3 to 7 illustrate the effect of ϵ in system's performance. In Figures 3 and 4, where the values of ε are greater than 30, the overshoot and settling time are clearly observed in both simulation and experimental results. These results show that an increase in the value of ε leads to an increase in the overshoot and a decrease in the settling time. The actuator of the experimental setup is a DC motor. The maximum input voltage is determined by the manufacturer to be less than 4.2 [V]. Therefore, the input saturation level can be considered to be 4.2. Hence, the maximum control input in Figures 3 and 4 are identical and are equal to 4.2[V]. Figures 3 and 4 also reveal that the controller performance is acceptable in the presence of saturation. In other words, actuator saturation does not destroy the stability of the system which is regarded as an advantage of the Controlled Lagrangian method.
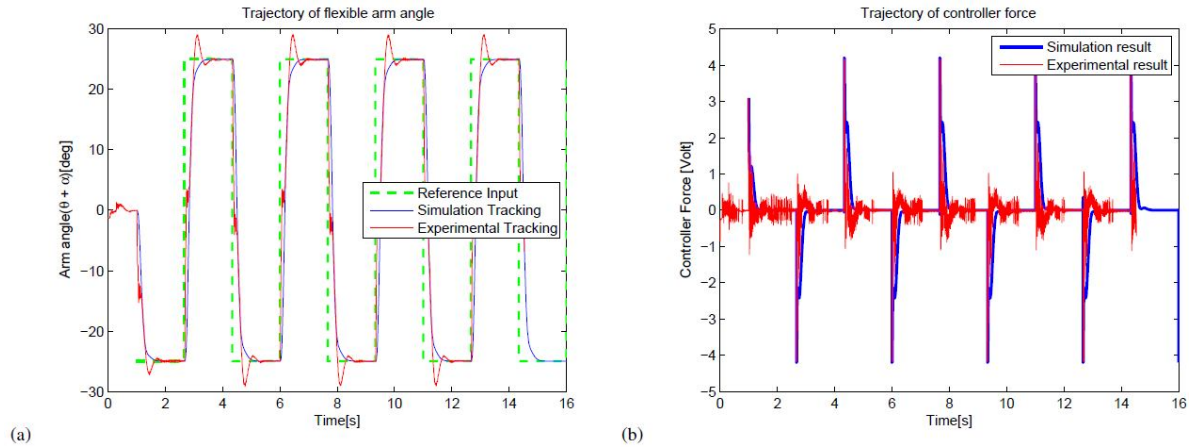
In Figures 5, 6 and 7, the value of ε is selected to be lesser than 30. A comparison between these figures show that the best performance in the experimental results is obtained for $\varepsilon = 20$ (Figure 5) where the overshoot is about 1 percent (0.5 degree) and the settling time is below one second (much better than the simulation). Figure 7 illustrates that for $\varepsilon < 20$ the experimental results as well as the simulation results show no overshoot, but the settling time is longer than a reasonable value. Moreover, these figures show that the maximum control effort decreases as ε reduces where we can use this property to prevent saturation.

Figures 5 and 8-10 illustrate the effect of c_0. As it was explained in (22), this coefficient indicates the dissipation rate of the system's energy. For small values of c_0, represented in figures 8 and 9, overshoots were observed. Small values of c_0 mean small dissipation rate in energy value; therefore, the presented overshoot is the direct result of an insignificant dissipation
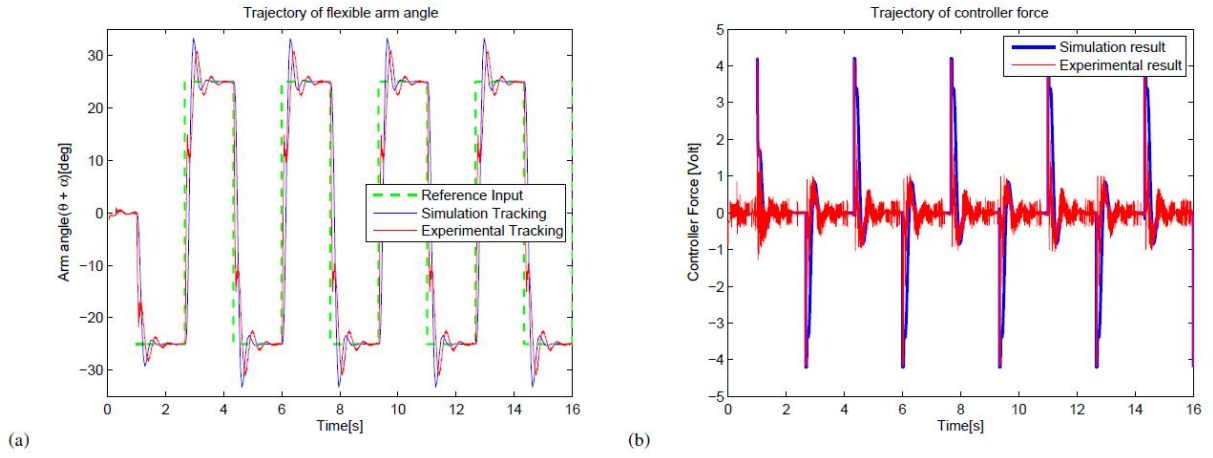
energy rate. On the other hand, Figure 10 clearly shows that the large values of c_0 dissipate energy more than the desired value which leads to the deterioration of settling time.

Implication of the partial feedback linearization method [31] on the flexible link system is depicted on Figure 11. Using data given in Table 1, the system is feedback linearized and the controller assigns gain coefficients to obtain closed-loop characteristics $\zeta = 0.6$, $\omega_n = 6.5$. To compare with the Controlled Lagrangian method, Figure 11 shows higher discrepancy between simulation and experiment. Furthermore, the trajectory and control input history of the experimental result are more sluggish for the partial feedback linearization method. The reason returns to the characteristics of feedback linearization that any uncertainty or model error prevents the cancellation of nonlinear expressions in the governing equations. In other words, the discrepancy and sluggish behavior of the experimental result is due to the fact that this method is highly sensitive to uncertainties and unknown parameters. On the contrary, as it is observed from Figures 2-10, the Controlled Lagrangian method enjoys from a robustness degree against unknown parameters and uncertainties.
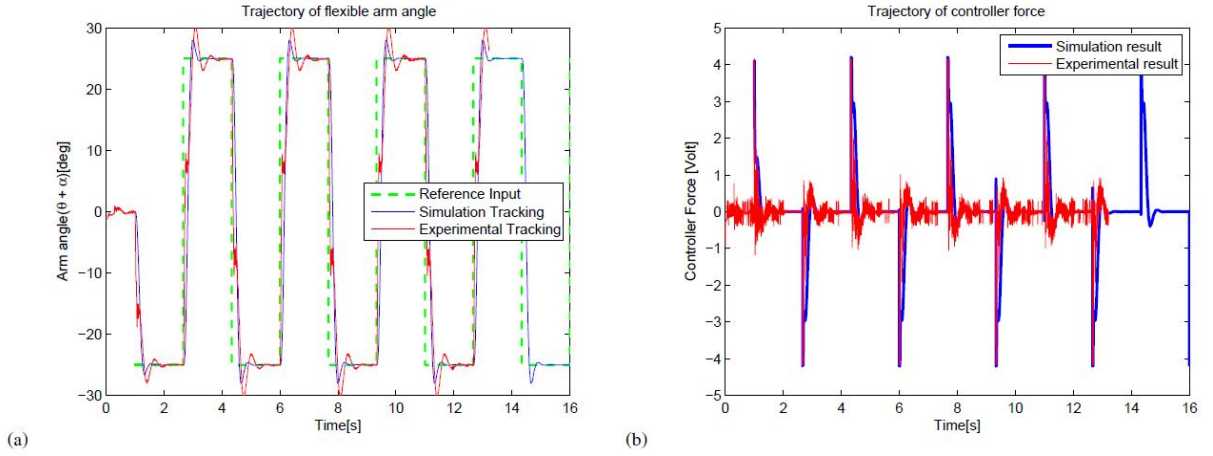
It should be noted that both methods use a model based approach to produce the control law. The reason that the partial feedback linearization method is sensitive to uncertainties while our proposed method is well robust can be explained by the usage of the model in each method. The partial feedback linearization method employs system's model to cancel the nonlinear terms of the governing equations of motion. Therefore, any difference between the model and the real system results in a residual nonlinear term that diminishes stability and performance. On the other hand, the Controlled Lagrangian method employs the model to design a control law that reduces mechanical energy of the system. In this perspective, the difference between parameters of the model and the real system is not a matter of great importance as long as the structure of expressions remains the same.
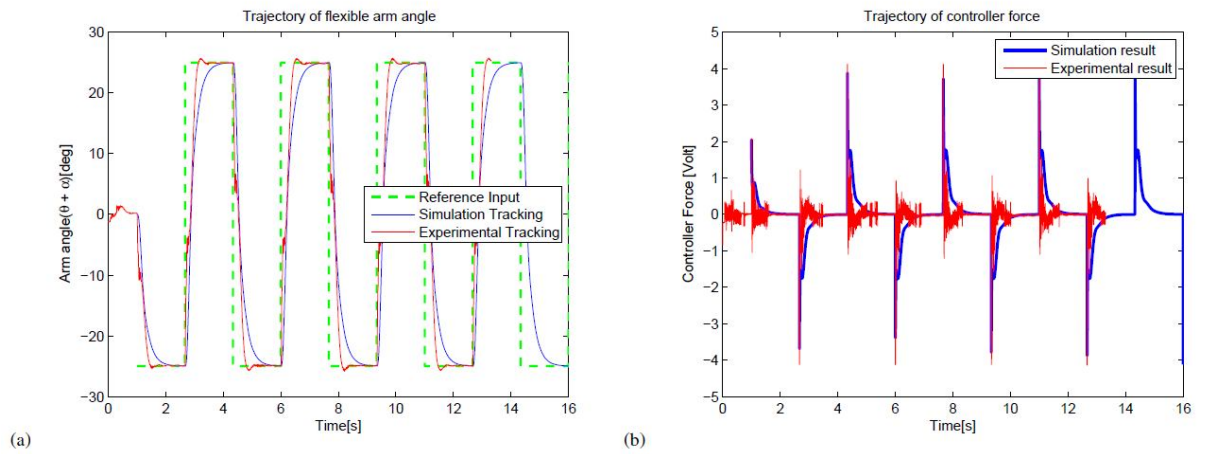

Fig 2: Simulation and experimental results for $\epsilon = 30$, $c_0 = 0.2$: (a) Tracking reference input; (b) Control effort
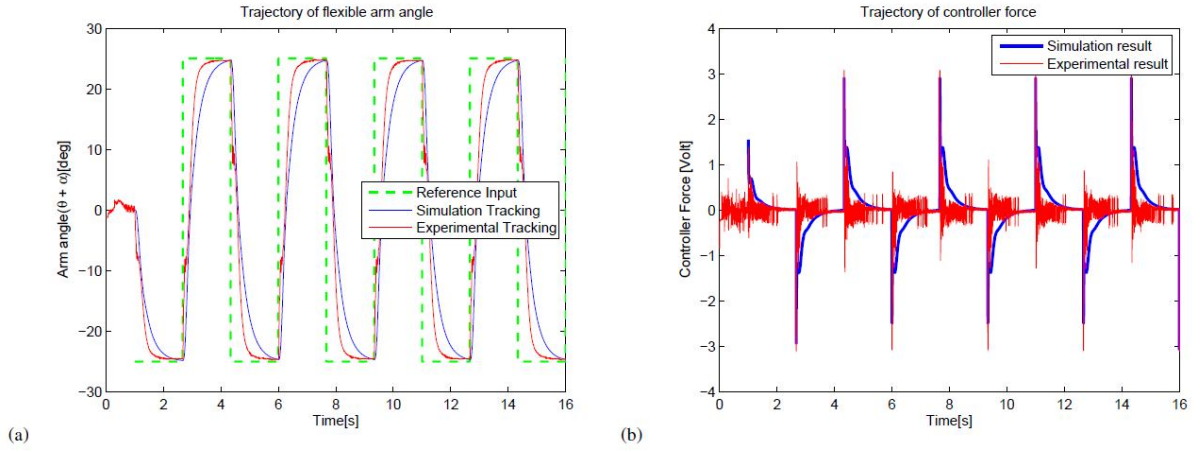
Fig 3: Simulation and experimental results for $\epsilon = 50$, $c_0 = 0.2$: (a) Tracking reference input; (b) Control effort
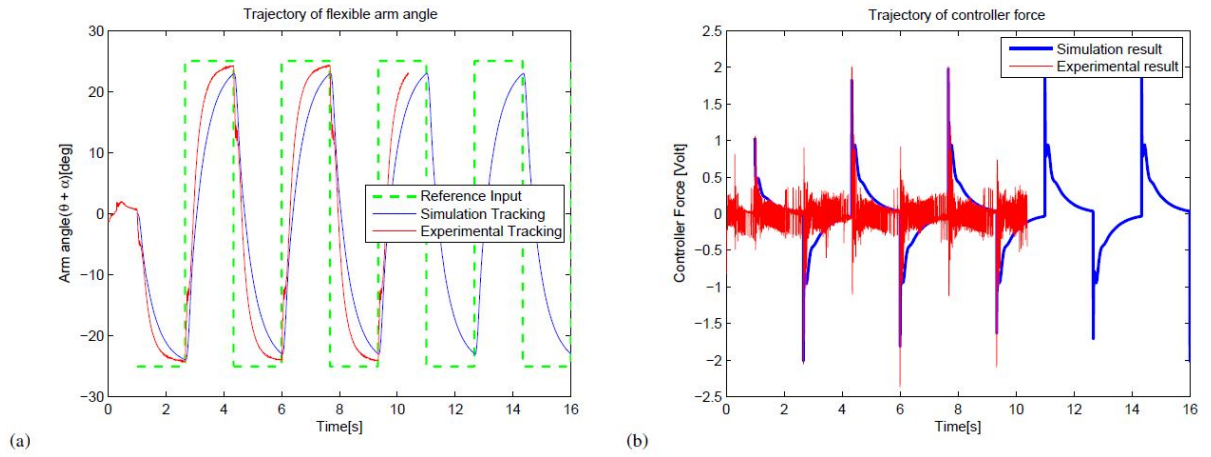

Fig 4: Simulation and experimental results for $\epsilon = 40$, $c_0 = 0.2$: (a) Tracking reference input; (b) Control effort
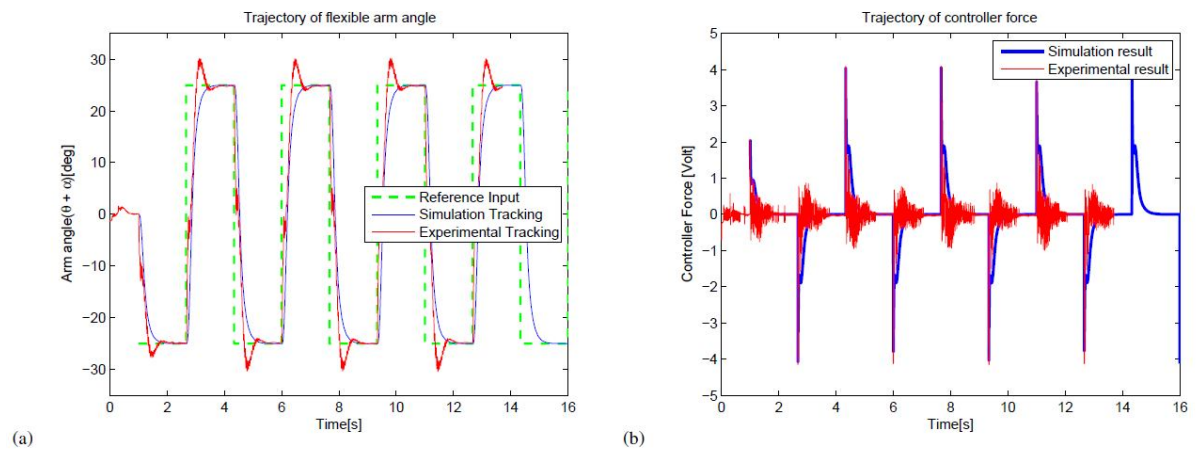

Fig 5: Simulation and experimental results for $\epsilon = 20$, $c_0 = 0.2$: (a) Tracking reference input; (b) Control effort

Fig 6: Simulation and experimental results for $\epsilon = 15$, $c_0 = 0.2$: (a) Tracking reference input; (b) Control effort
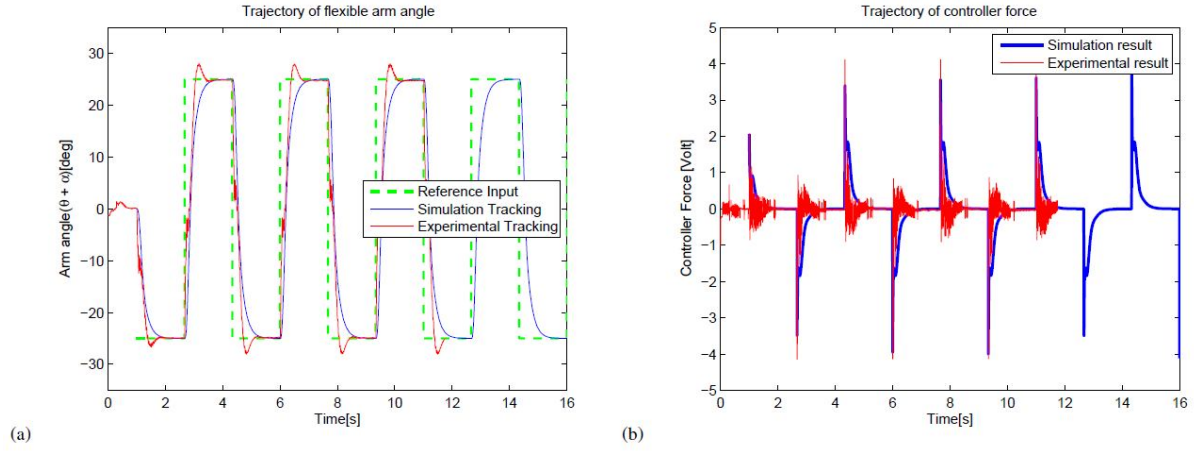

Fig 7: Simulation and experimental results for $\epsilon = 10$, $c_0 = 0.2$: (a) Tracking reference input; (b) Control effort
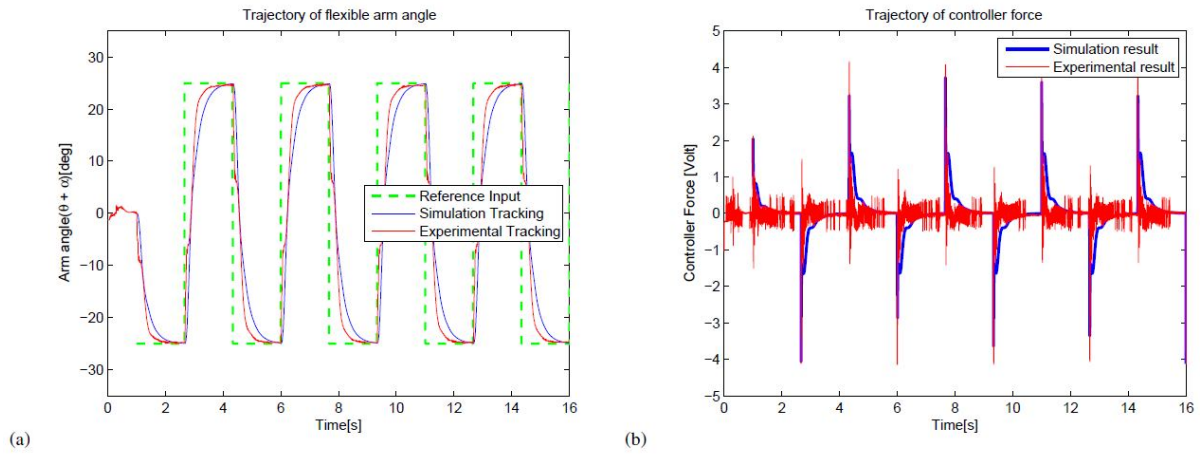

Fig 8: Simulation and experimental results for $\epsilon = 20$, $c_0 = 0.15$: (a) Tracking reference input; (b) Control effort

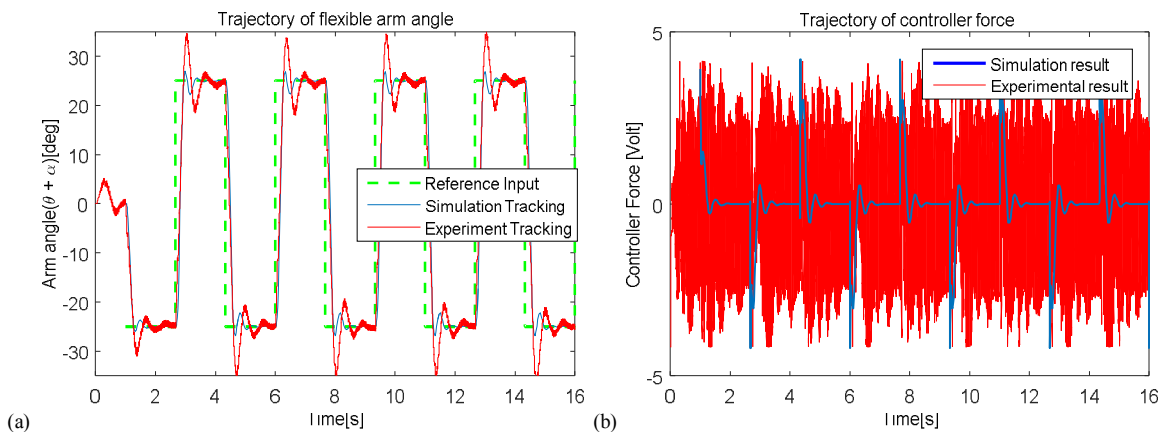(a)   (b)

Fig 9: Simulation and experimental results for $\epsilon = 20$, $c_0 = 0.17$: (a) Tracking reference input; (b) Control effort

(a)   (b)

Fig 10: Simulation and experimental results for $\epsilon = 20$, $c_0 = 0.25$: (a) Tracking reference input; (b) Controller force

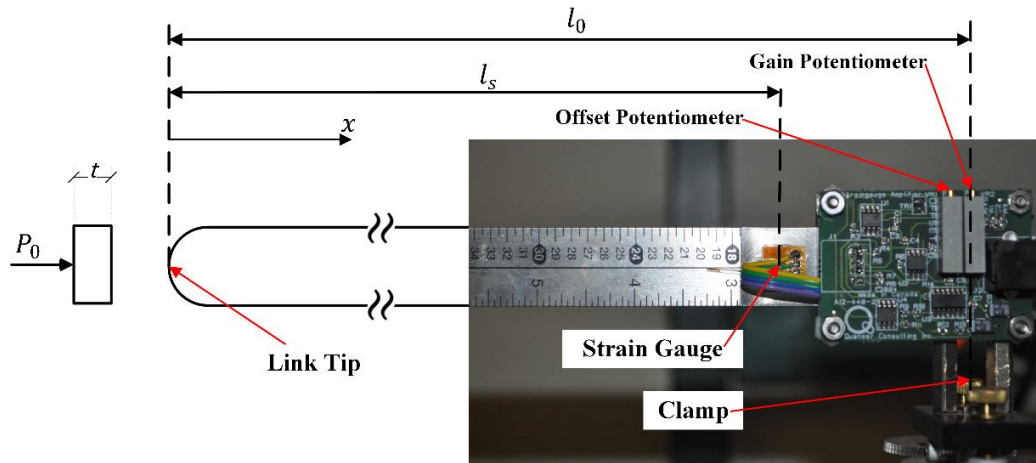(a)   (b)

Fig 11: Simulation and experimental result for partial feedbalck linearization: (a) Tracking reference input; (b) Controller force

6. Conclusion

This sequel presented a theoretical and experimental study about the Controlled Lagrangian method to control a laboratory flexible link device. It was shown that the method could be used to apply a direct control on the maximum value of the input that can be employed to avoid input saturation. Also, it was illustrated that gain tuning can be employed by regulating controller gains with respect to their role in the artificial system's energy. This is of particular importance for online tuning of the controller's gain. Additionally, a comparison between the Controlled Lagrangian method and the partial feedback linearization method reveals that the Controlled Lagrangian method is able to attenuate the effects of uncertainties on control performance while the partial feedback linearization method fails to do that. The experimental results indicated that the reference input can be well tracked by adopting this control strategy.

Appendix A- Measurement of tip deflection by strain gauge

This appendix explains the method that was used to measure tip deflection by means of a strain gauge sensor. As it can be seen from Figure A.1, the sensor is attached close to the clamped edge of the link. Link's length is l_0 and the distance between the tip of the link and the strain gauge is l_s. The values of l_0 and l_s are given in Table 1.

Fig A. 1: Tip deflection measuring details of flexible link

For a constant force P_0 acting at the link tip, it is known that the tip's deflection δ is

$$\delta = \frac{P_0 l_0^3}{3EI} \tag{A.1}$$

where E and I denote elastic modulus and second moment of area of the link. This force produces moment $M_0 = P l_0$ at the clamp. Solving (A.1) for elastic modulus results in

$$E = \frac{P_0 l_0^3}{3\delta I} \tag{A.2}$$

Assuming the first mode shape, the cantilever link of Figure A.1 is acting like a beam in bending. The stress σ experienced on the surface of the beam in bending is given by,

$$\sigma(x) = E\varepsilon(x) = \frac{M(x)t}{2\,I} \tag{A.3}$$

where t is the thickness of the beam. Using (A.2) to solve (A.3) for the strain at $x = l_s$, it is obtained that,

$$\varepsilon(l_s) = \frac{M(l_s)t}{2EI} = \frac{P_0 l_s t}{2I} \frac{3\delta I}{P_0 l_0^3} = \frac{3t l_s}{2l_0^3}\delta \tag{A.4}$$

Expression (A.4) represents a linear relationship between tip deflection δ and strain value at $x = l_s$. The calibration process of the strain gauge employs two adjustable potentiometers as it is depicted in Figure A.1. First, one should put the flexible link in rest position. In this position, output voltage of strain gauge should be zero. If the voltage, measured by a voltmeter, shows other values, one should adjust the Offset potentiometer to make the output voltage zero. After that, it is necessary to check that the device works linearly for the prospective deflection value. The sensor should read 1 Volt per 1 inch of tip deflection [29]. If for 1 inch deflection the sensor reads other values, one should gently adjust the gain potentiometer until the sensor reads 1 Volt.

References

[1] J.M. Martins, Z. Mohamed, M.O. Tokhi, J.S.a. Da Costa, M.A. Botto, Approaches for dynamic modelling of flexible manipulator systems, IEE Proceedings-Control Theory and Applications, 150 (2003) 401-411.

[2] G. Naganathan, A. Soni, An analytical and experimental investigation of flexible manipulator performance, in: Robotics and Automation. Proceedings. 1987 IEEE International Conference on, IEEE, 1987, pp. 767-773.

[3] E. Soltani, M. Naraghi, Inversion-based nonlinear end-tip control of flexible arm in presence of large model uncertainties, in: Robotics, Automation and Mechatronics, 2006 IEEE Conference on, IEEE, 2006, pp. 1-6.

[4] D.P. Magee, W.J. Book, Eliminating multiple modes of vibration in a flexible manipulator, in, Georgia Institute of Technology, 1993.

[5] Z.H. Luo, Direct strain feedback control of flexible robot arms: new theoretical and experimental results, IEEE Transactions on Automatic Control, 38 (1993) 1610-1622.

[6] A.M. Bloch, N.E. Leonard, J.E. Marsden, Stabilization of mechanical systems using controlled Lagrangians, in: Decision and Control, 1997., Proceedings of the 36th IEEE Conference on, IEEE, 1997, pp. 2356-2361.

[7] A.M. Bloch, N.E. Leonard, J.E. Marsden, Matching and stabilization by the method of controlled Lagrangians, in: Decision and Control, 1998. Proceedings of the 37th IEEE Conference on, IEEE, 1998, pp. 1446-1451.

[8] A.M. Bloch, N.E. Leonard, J.E. Marsden, Controlled Lagrangians and the stabilization of mechanical systems. I. The first matching theorem, IEEE Transactions on automatic control, 45 (2000) 2253-2270.

[9] A.M. Bloch, D.E. Chang, N.E. Leonard, J.E. Marsden, Controlled Lagrangians and the stabilization of mechanical systems. II. Potential shaping, IEEE Transactions on Automatic Control, 46 (2001) 1556-1571.

[10] D. Auckly, L. Kapitanski, W. White, Control of nonlinear underactuated systems, Communications on Pure and Applied Mathematics: A Journal Issued by the Courant Institute of Mathematical Sciences, 53 (2000) 354-369.

[11] D. Auckly, L. Kapitanski, On the λ-equations for matching control laws, SIAM Journal on control and optimization, 41 (2002) 1372-1388.

[12] F. Andreev, D. Auckly, S. Gosavi, L. Kapitanski, A. Kelkar, W. White, Matching, linear systems, and the ball and beam, Automatica, 38 (2002) 2147-2152.

[13] D.E. Chang, A.M. Bloch, N.E. Leonard, J.E. Marsden, C.A. Woolsey, The equivalence of controlled Lagrangian and controlled Hamiltonian systems, ESAIM: Control, Optimisation and Calculus of Variations, 8 (2002) 393-422.

[14] A. Donaire, R. Mehra, R. Ortega, S. Satpute, J.G. Romero, F. Kazi, N.M. Singh, Shaping the energy of mechanical systems without solving partial differential equations, in: American Control Conference (ACC), 2015, IEEE, 2015, pp. 1351-1356.

[15] A. Albu-Schäffer, C. Ott, F. Petit, Energy Shaping Control for a Class of Underactuated Euler-Lagrange Systems, in: SyRoCo, 2012, pp. 567-575.

[16] J. Xie, B. Sun, W. Wei, Z. Liu, Application Kinetic Energy Shaping to Controlling and Anticontrolling Chaotic Gait of Underactuated Compass-Gait Bipedal Robot, in: ASME 2017 International Design Engineering Technical Conferences and Computers and Information in Engineering Conference, American Society of Mechanical Engineers, 2017.

[17] G. Lv, R.D. Gregg, Towards total energy shaping control of lower-limb exoskeletons, in: American Control Conference (ACC), 2017, IEEE, 2017, pp. 4851-4857.

[18] R. Ortega, M.W. Spong, F. Gomez-Estern, G. Blankenstein, Stabilization of underactuated mechanical systems via interconnection and damping assignment, IEEE Trans. Aut. Control, (2000).

[19] R. Ortega, M.W. Spong, F. Gómez-Estern, G. Blankenstein, Stabilization of a class of underactuated mechanical systems via interconnection and damping assignment, IEEE transactions on automatic control, 47 (2002) 1218-1233.

[20] R. Ortega, A. Van Der Schaft, B. Maschke, G. Escobar, Interconnection and damping assignment passivity-based control of port-controlled Hamiltonian systems, Automatica, 38 (2002) 585-596.

[21] C.F. Aguilar-Ibañez, O.O.G. Frias, A simple model matching for the stabilization of an inverted pendulum cart system, International Journal of Robust and Nonlinear Control: IFAC-Affiliated Journal, 18 (2008) 688-699.

[22] A. Sanz, V. Etxebarria, Interconnection and damping assignment passivity-based experimental control of a single-link flexible robot arm, in: Computer Aided Control System Design, 2006 IEEE International Conference on Control Applications, 2006 IEEE International Symposium on Intelligent Control, 2006 IEEE, IEEE, 2006, pp. 2504-2509.

[23] N.K. Haddad, A. Chemori, S. Belghith, Robustness enhancement of IDA-PBC controller in stabilising the inertia wheel inverted pendulum: theory and real-time experiments, International Journal of Control, (2017) 1-16.

[24] A. Donaire, J.G. Romero, R. Ortega, B. Siciliano, M. Crespo, Robust IDA-PBC for underactuated mechanical systems subject to matched disturbances, International Journal of Robust and Nonlinear Control, 27 (2017) 1000-1016.

[25] J. Ferguson, A. Donaire, R. Ortega, R.H. Middleton, Matched disturbance rejection for energy-shaping controlled underactuated mechanical systems, in: Decision and Control (CDC), 2017 IEEE 56th Annual Conference on, IEEE, 2017, pp. 1484-1489.

[26] J. José, E. Saletan, Classical dynamics: a contemporary approach, in, First ed. Cambridge University Press, UK. , 2000.

[27] J.E. Marsden, Lectures on mechanics, Cambridge University Press, 1992.

[28] F. Bellezza, L. Lanari, G. Ulivi, Exact modeling of the flexible slewing link, in: Robotics and Automation, 1990. Proceedings., 1990 IEEE International Conference on Robotics and Automation, IEEE, 1990, pp. 734-739.

[29] Quanser Consulting Inc, SRV02-Series: Flexible Link Handout, in, Ontario, Canada, 2009.

[30] M. Hemmasian Ettefagh, M. Naraghi, M. Mahzoon, Robustness of Controlled Lagrangian Method to the Structured Uncertainties, AUT Journal of Mechanical Engineering, 2 (2018) 61-72.

[31] A. Arisoy, M. Gokasan, O. Bogosyan, Partial feedback linearization control of a single flexible link robot manipulator, in: Recent Advances in Space Technologies, 2005. RAST 2005. Proceedings of 2nd International Conference on Recent Advances in Space Technologies, IEEE, 2005, pp. 282-287.